



LUND UNIVERSITY

Exploration of Supraventricular Conduction with respect to Atrial Fibrillation. Methodological Aspects on Selected Techniques

Carlson, Jonas

2005

[Link to publication](#)

Citation for published version (APA):

Carlson, J. (2005). *Exploration of Supraventricular Conduction with respect to Atrial Fibrillation. Methodological Aspects on Selected Techniques*. [Doctoral Thesis (compilation), Cardiology]. Department of Clinical Sciences, Lund University.

Total number of authors:

1

General rights

Unless other specific re-use rights are stated the following general rights apply:

Copyright and moral rights for the publications made accessible in the public portal are retained by the authors and/or other copyright owners and it is a condition of accessing publications that users recognise and abide by the legal requirements associated with these rights.

- Users may download and print one copy of any publication from the public portal for the purpose of private study or research.
- You may not further distribute the material or use it for any profit-making activity or commercial gain
- You may freely distribute the URL identifying the publication in the public portal

Read more about Creative commons licenses: <https://creativecommons.org/licenses/>

Take down policy

If you believe that this document breaches copyright please contact us providing details, and we will remove access to the work immediately and investigate your claim.

LUND UNIVERSITY

PO Box 117
221 00 Lund
+46 46-222 00 00

Modification of Intrinsic AV-Nodal Properties by Magnesium in Combination With Glucose, Insulin, and Potassium (GIK) During Chronic Atrial Fibrillation

M. P. Ingemansson, MD, J. Carlson, MSc, and S. B. Olsson, MD, PhD

Abstract: *Objective:* To explore the effects of $MgSO_4$ in combination with glucose, insulin, and potassium (GIK) on intrinsic AV-nodal properties during chronic atrial fibrillation. *Methods:* The study included two patient groups—(a) control and intervention and (b) intervention—with different infusion times and concentrations of $MgSO_4$. Ambulatory electrocardiographic recordings were analyzed using modified heart-rate stratified histogram (HRSH) analysis allowing detailed observation of the RR distribution at different average heart rate levels. The two RR-interval populations observed in most patients were characterized by analyzing the relationship between the summits of the peaks of the bimodal histograms. *Results:* A bimodal RR distribution with a shorter and a longer RR-interval population was observed in 9 of 11 (control), 9 of 11 (intervention) in group (a), and 11 of 13 in group (b) patients. No significant changes in the two RR populations were seen in the control registration (group a). There were, however, indications of a conduction delay in the longer RR intervals in group (a), which received a low concentration of $MgSO_4$, when control was compared with intervention recordings. In group (b), receiving a high $MgSO_4$ concentration, a conduction delay was seen in both the shorter and longer RR populations, being most pronounced for the longer RR population. *Conclusion:* High $MgSO_4$ levels caused a delay in both the shorter and longer RR intervals. The conduction delay in the longer RR population was most pronounced, indicating that $MgSO_4$ differently affected the two corresponding AV-nodal pathways. **Key words:** ambulatory ECG recording, atrial fibrillation, AV node, fast pathway, magnesium, RR interval, slow pathway.

Nearly 50 years ago, Moe et al. found evidence of a dual AV-nodal conduction system (1). The longitudinal dissociation of two separate pathways within the AV node has been confirmed in both animals and

humans (2,3). Once the excitation waves have entered the AV node, transmission through the so-called slow and fast pathways is known to be affected by decremental conduction, cancellation, augmentation, and echo phenomena and will at any given moment be modulated with great precision by autonomic nervous discharge (4–7). Later experimental works have indicated that AV-nodal transmission is also dependent on the pattern of AV-nodal input (8–11).

From the Department of Cardiology, Lund University, Lund, Sweden.
Reprint requests: M. P. Ingemansson, MD, Department of Cardiology, University Hospital, S-221 85 Lund, Sweden.
Copyright © 1998 by Churchill Livingstone®
0022-0736/98/3104-0003\$5.00/0

Previous microelectrode studies of AV-nodal conduction have shown that there is a dual AV-nodal input, and the atrionodal input routes represent conduction from the interatrial septum and conduction along the crista terminalis into the AV node, respectively (8).

Although the multiple re-entrant circuits in the fibrillating atrium transmit rapid and irregular depolarizing wavelets to the AV-nodal region, heart-rate stratified histogram (HRS) analysis from ambulatory electrocardiographic (ECG) recordings reveal an output with a distinct bimodal distribution of RR intervals in most patients (12–14).

On the basis of both invasive (13,15) and noninvasive studies (12,14), it has been suggested that one RR population represents AV-nodal conduction at the anterosuperior perinodal tissue, proximal to the His bundle, and the other, conduction in the posterior AV-nodal approaches, close to the tricuspid annulus.

The transmission of atrial impulses through the nodal region during chronic atrial fibrillation (CAF) is dependent on the conduction velocity and refractory period at the AV node, the main electrophysiologic determinants of the ventricular rate and thereby of the RR-interval distribution during CAF (16). It has been proposed that the two distinct AV-nodal pathways differ in conduction and refractory characteristics and might therefore be affected differently by pharmacological intervention (17).

Based on considerations regarding the pathoelectrophysiology of the fibrillating atrial myocardium (18–22), we have analyzed the effects of $MgSO_4$ and GIK solution on the atrial myocardium during pacing (23) and fibrillation (24). Although these interventions may have beneficial antiarrhythmic properties in addition to their verified effects during sinus rhythm (25,26), detailed information about the effect of $MgSO_4$ and GIK solution on AV-nodal conduction during CAF is lacking. The aim of this study was therefore to evaluate the effects of $MgSO_4$ and glucose, insulin, and potassium (GIK) solution on intrinsic AV-nodal function. For this purpose, we studied their effects on the two RR-interval populations, which can be observed on HRS analysis in most patients with CAF, and which most likely represent conduction via the dual AV-nodal pathways (12–15).

Methods

Patient Groups and Interventions

Two patient groups, (a) and (b), were included in the study (Fig. 1). Both control and intervention recordings were performed in group (a), whereas

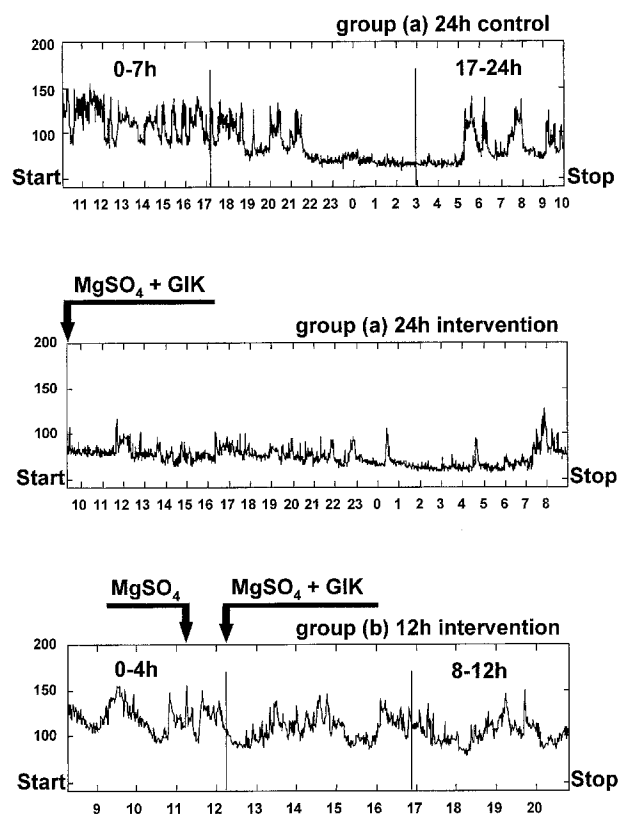


Fig. 1. Holter recordings from one typical patient in the control and intervention recordings in group (a) and from one patient in group (b). The x axis shows the time of day and the y axis the heart rate. A 24-hour Holter recording was performed in group (a) (control and intervention), and a 12-hour recording in group (b) (intervention). Comparison was made between hours 0 to 7 and 17 to 24 in the control recordings in group (a) and between the whole 24-hour registration of the control and intervention recordings in group (a), as the same patient material was used. Comparison was made between hours 0 to 4 and 8 to 12 in group (b). The autonomic influence on AV-nodal conduction prompted us to study the distribution of RR intervals at different levels of autonomic nervous discharge by making observations at well-defined average heart-rate levels.

only intervention recordings were performed in group (b). Group (a) consisted of 9 men and 2 women, average age 64 ± 11 years. In group (b), there were 10 men and 3 women, average age 68 ± 8 years. There were no significant differences in age and gender between the two groups. All patients included had CAF with duration of more than 3 months. In group (a), pharmacological treatment had been unsuccessful in terminating the arrhythmia, and DC conversion had not been attempted. In group (b), both pharmacological treatment and DC conversion had been unsuccessful in terminating the arrhythmia. The same exclusion criteria were

used in both groups: diabetes mellitus, hyperthyroidism, renal or hepatic diseases, infections, or severe electrolyte disturbances. All antiarrhythmic treatment, including digoxin, was withdrawn at least 5 $T_{1/2}$ before participation in the study.

No infusates were given during the control registration in group (a). The intervention in the same group was performed 1 to 5 days later and consisted of a 24-hour infusion with 2,000 mL glucose (100 g/L⁻¹), MgSO₄ (100 mmol/L⁻¹), 40 IU/L⁻¹ of Actrapid, and K⁺ supplement (80 mmol/L⁻¹), if S-K was below 4.0 mmol/L⁻¹ at the start. In group (b), a higher dose of MgSO₄ and a shorter infusion time was used. Three hours after start of the recording, a bolus infusion of 0.15 mmol/kg⁻¹ of MgSO₄ was given over 10 minutes in 250 mL glucose (50 g/L⁻¹). The MgSO₄ and GIK maintenance infusion was started after 4 hours of recording and was given over 8 hours. It consisted of 1,000 mL glucose (100 g/L⁻¹), MgSO₄ (0.1 mmol/kg⁻¹/hr⁻¹), Actrapid 20 IU/L⁻¹, and K⁺ supplement (40 mmol/L⁻¹), if S-K was below 4.0 mmol/L⁻¹ at the start. The MgSO₄ and GIK solutions were administered via a peripheral vein.

The investigation conforms to the principles outlined in the Declaration of Helsinki (BMJ 1964;ii:177). The study was approved by the Ethical Committee of the Medical Faculty, Lund University, Sweden, approval numbers LU 134-94, LU 15-96.

ECG Recording and Analysis

The ECG recordings were performed using a model 423 Dynacord Holter cassette recorder. The electrode configuration consisted of two V leads, consistent with typical, 2-channel Holter recording (423 Dynacord; Del Mar Avionics, Irvine, CA), as well as a modified lead III on the third channel. Soft, flexible electrodes were used. In group (a), ECG recordings were performed over 24 hours and the whole periods of control and intervention recordings were compared to each other. In addition, the first 7 hours (0–7) of the recording in the control registrations were compared with the last 7 hours (17–24). In group (b), the recordings were continued for 12 hours and the first 4 hours (0–4) of recording were compared with the last 4 hours (8–12) (Fig. 1).

The ECG was analyzed with a model 263 StrataScan Holter analysis system with a resolution of 15 to 16 ms, and it was also carefully analyzed by visual inspection, to make sure that only AF with narrow QRS complexes was included. Afterward, the lengths of all RR intervals were saved onto a

5 $\frac{1}{4}$ -inch floppy disc and analyzed on a computer running a specially developed MATLAB®-based program. The methodologic aspects of the RR-interval pooling procedure have been described elsewhere (14), but the following modifications were made. The entire series of RR-intervals was divided into sequences of 20 individual RR intervals as follows, 1–20, 2–21, 3–22 . . . (Fig. 2). Each sequence was then pooled into different heart-rate levels, according to its average heart rate (eg, 45–50, 50–55, 55–60 beats per minute [bpm], etc.). Histograms were constructed of the individual RR-interval values at each heart-rate level. Each histogram bar had a width of 15 to 16 ms, corresponding to the resolution of the StrataScan system.

Each histogram was analyzed by the computer with regard to the number of distinct populations of RR intervals (peaks). Each point at which the slope of the histogram changed from positive to negative was considered a peak. If the distance between 2 peaks was less than 3 bars (<50 ms), this was considered a ripple in the histogram, and a smoothing procedure was used in which the value for each bar was recalculated as the average between its original value and that of one bar on each side. The smoothing procedure was repeated until no peaks were closer to each other than 50 ms. The remaining peaks were considered to belong to different RR-interval populations (Fig. 2). The peak locations of the RR-interval populations were estimated by fitting a second-degree polynomial to the highest bar and the 2 adjacent bars on each side. The highest and second-highest peaks were classified as dominant and nondominant, respectively. The quotient of and distance between the peak locations of the longer and shorter RR population were calculated as the peak value ratio (PVR) and peak gap [PG(ms)], respectively (Fig. 2). At lower heart-rate levels, the peak corresponding to the longer RR-interval population [PV(s)] is dominant. As the heart rate increases, the peak of the shorter RR-interval population [PV(f)] will increase and become dominant. The heart-rate level at which a change in peak dominance was seen was called the peak dominant change (PDC). PVR, PG, PV(f), and PV(s) were calculated at the PDC.

Statistical Evaluation

Data are expressed as medians (tables), means and standard deviations (SD) from the mean (text + tables). Friedman's Test for repeated measurements was used for statistical evaluation of the whole group. Wilcoxon's signed rank test was used

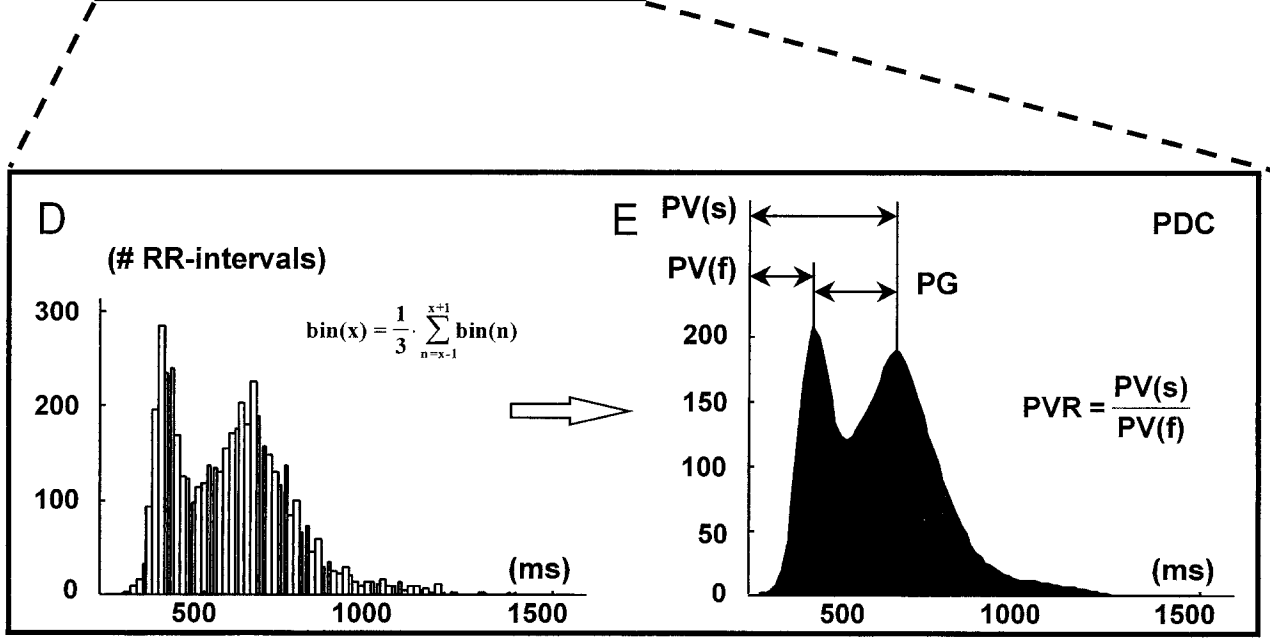
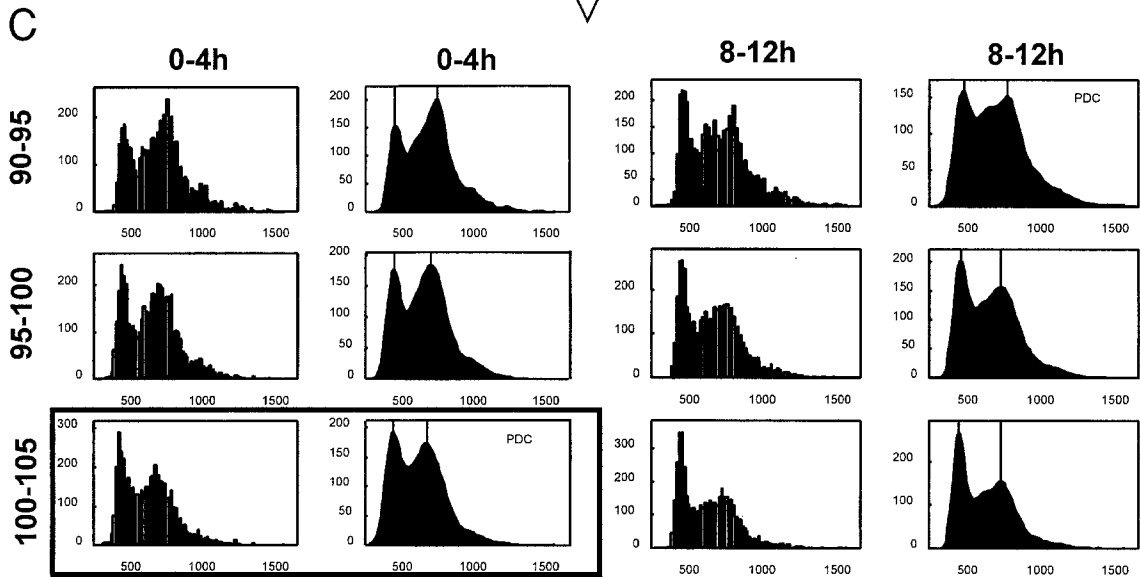
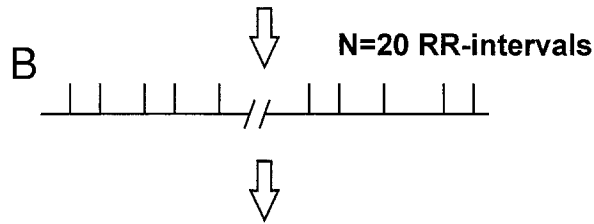
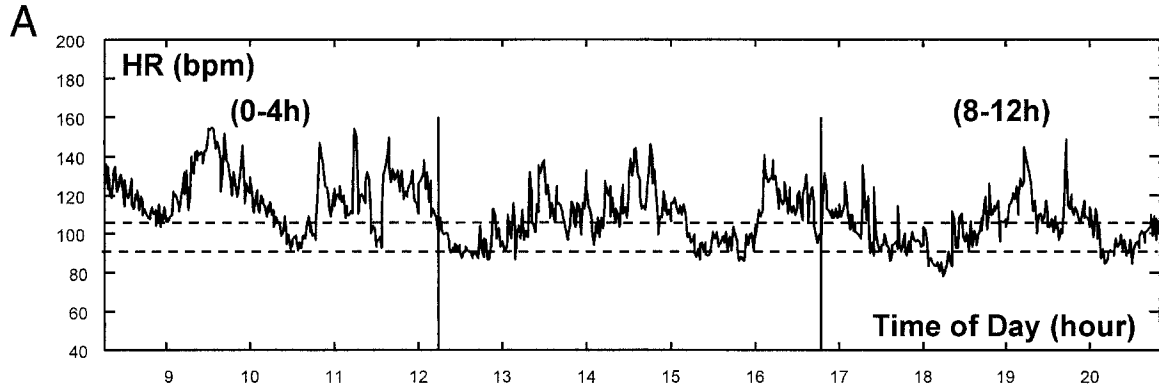


Table 1. Peak Indices for the Control Group, Comparing the First Seven Hours (0–7) with the Last Seven Hours (17–24)

Case	PDC (HR level)		PG (ms) at PDC		PVR at PDC		PV(f) (ms) at PDC		PV(s) (ms) at PDC	
	0–7 hr	17–24 hr	0–7 hr	17–24 hr	0–7 hr	17–24 hr	0–5 hr	17–24 hr	0–5 hr	17–24 hr
1	MV	120	MV	184	MV	1.48	MV	381	MV	565
2	105	100	245	246	1.65	1.62	377	394	622	640
3	100	95	257	261	1.61	1.60	424	436	681	697
4	115	120	157	138	1.36	1.31	437	444	594	582
5	105	100	179	193	1.41	1.43	433	451	612	644
6	125	115	100	159	1.26	1.37	387	426	487	585
7	UM	UM	0	0	1.00	1.00	UM	UM	UM	UM
8	115	120	157	100	1.39	1.25	406	408	563	508
9	110	105	166	155	1.38	1.36	437	434	604	589
10	110	115	86	165	1.19	1.38	454	434	540	599
11	UM	UM	0	0	1.00	1.00	UM	UM	UM	UM
Median	110	115	157	159	1.37	1.37	429	434	599	589
Mean (SD)	111 (8)	110 (10)	122 (93)	146 (85)	1.33 (0.2)	1.35 (0.2)	419 (27)	423 (24)	588 (58)	601 (54)
<i>P</i> value	NS		NS		NS		NS		NS	

HR, heart rate; h, hours; ms, milliseconds; MV, missing value; NS, nonsignificant; PV(f), peak value of the shorter RR-interval population; PV(s), peak value of the longer RR-interval population; PDC, peak dominant change; PG, peak gap; PVR, peak value ratio; SD, standard deviation; UM, unimodal.

as a post hoc test to evaluate the significance of changes within the groups. *P* values were considered significant if $P < .05$ (*).

Results

HRS Analysis

In the control registrations in group (a), peaks representing the shorter and longer RR-interval populations [PV(f) and PV(s)] could be distinguished in 9 of 11 patients in the whole 24-hour registration and in both shorter registrations (0–7 hr and 17–24 hr) (Tables 1 and 2). There was a shift in dominance between the two RR-interval populations, and consequently PDC, PG, PVR, PV(f), and PV(s) could be estimated in all these nine patients. The PDC location in the first patient (Table 1) could not be determined in the 0- to 7-hour registration,

because heart-rate variability was low. However, the heart-rate variability increased, and the PDC location could be determined in the 17- to 24-hour registration. The remaining two patients had a unimodal RR-interval distribution and PDC could not be calculated. Based on earlier observations (2), these were regarded as 2 superimposed RR populations, and PG and PVR were therefore given the values 0 and 1, respectively. The change in dominance occurred at average heart-rate levels ranging from 100 to 125 (0–7 hr) and from 95 to 120 bpm (17–24 hr) for the shorter registration periods, and from 100 to 130 for the whole 24-hour registration. No significant changes were seen in PDC location, PG, PVR, PV(f), and PV(s) when comparison was made between the first 7-hour registration (0–7 hr) and the last 7-hour registration (17–24 hr) (Table 1).

Following intervention with MgSO₄ and GIK infusion in group (a), (low MgSO₄ concentration),

Fig. 2. Schematic illustration of the method used for studying the two RR-interval populations. **(A)** A 12-hour ambulatory electrographic recording from one patient in group (b). Each QRS complex is identified, and all RR intervals in the recording are calculated. The black bars indicate the 0 to 4 and 8 to 12 hour periods. **(B)** The entire series of RR intervals was divided into sequences of 20 individual RR intervals. One step movement (ie, 1–21, 2–22) created the sequences, and the average heart rate was calculated for each sequence. **(C)** All individual RR intervals within sequences were pooled into histograms at different heart-rate levels, calculated from the average of the 20 consecutive RR intervals. Thus, RR intervals with the same average heart rate are pooled into the same histogram. Only heart-rate levels from 90 to 105 bpm are illustrated. **(D)** Using the formula shown smooths the original histogram. **(E)** The find-peak function could, with great precision, estimate the position of the two RR-interval populations in the smoothed histogram. PV(f), peak value of the shorter RR-interval population (ms, x axis). PV(s), peak value of the longer RR-interval population (ms, x axis). PG, peak gap (ie, the distance between the two RR populations) (ms, x axis). PVR, peak value ratio (ie, the quotient of the longer and shorter RR-interval populations). All peak indices were estimated at the heart-rate level where the peak dominance changed.

Table 2. Peak Indices for Group (a) (Control + Intervention), Comparing Recordings of the Whole 24-Hour Control Period With the 24-Hour Intervention Period in Group (a)

Case	PDC (HR level)		PG (ms) at PDC		PVR at PDC		PV(f) (ms) at PDC		PV(s) (ms) at PDC	
	Control	Interv	Control	Interv	Control	Interv	Control	Interv	Control	Interv
1	120	70	169	187	1.43	1.27	389	688	558	875
2	100	95	245	273	1.63	1.73	387	376	632	649
3	100	95	258	253	1.61	1.55	424	460	682	713
4	120	110	153	136	1.37	1.29	417	468	570	604
5	105	110	175	197	1.40	1.49	438	405	613	602
6	130	130	102	116	1.27	1.31	378	378	480	494
7	UM	UM	0	0	1.00	1.00	UM	UM	UM	UM
8	115	105	147	173	1.36	1.39	409	440	556	613
9	115	110	117	156	1.28	1.37	420	425	537	581
10	110	110	87	111	1.19	1.24	455	456	542	567
11	UM	UM	0	0	1.00	1.00	UM	UM	UM	UM
Median	115	110	147	156	1.36	1.31	417	440	558	604
Mean (SD)	113 (10)	104 (16)	132 (84)	146 (88)	1.32 (0.2)	1.33 (0.2)	413 (25)	455 (94)	574 (60)	633 (108)
P value	P = .05		P < .05		NS		NS		P < .05	

HR, heart rate; interv, intervention; ms, milliseconds; NS, nonsignificant; PV(f), peak value of the shorter RR-interval population; PV(s), peak value of the longer RR-interval population; PDC, peak dominant change; PG, peak gap; PVR, peak value ratio; SD, standard deviation; UM, unimodal.

shorter and longer RR-interval populations could be distinguished in 9 of 11 patients (Table 2). The remaining two patients had a unimodal RR-interval distribution, and the PDC could not be calculated. Once again, the PG and PVR were given the values 0 and 1, respectively, in these 2 cases. The PDC occurred at average heart-rate levels ranging from 70 to 130. No significant change was seen in PDC location when comparing the control and the intervention recordings in group (a), although the mean value decreased from 113 bpm (control) to 104 bpm (intervention) ($P = .05$) (Table 2). The PV(f) and PVR at the PDC were unaffected, whereas the PG

and PV(s) showed a significant increase, from 132 to 146 ms ($P < .05$) and from 574 to 633 ms ($P < .05$), respectively.

In group (b) (high $MgSO_4$ concentration), shorter and longer RR-interval populations could be distinguished in both shorter registration periods (0–4 hr and 8–12 hr) in 11 of 13 patients (Table 3). The remaining two patients had a unimodal RR-interval distribution in at least one of the registrations and the PDC could not be calculated. As before, the PG and PVR were given the values 0 and 1, respectively. In the 11 patients in whom both RR-interval populations could be discerned, the PDC occurred

Table 3. Peak Indices for Group (b), Comparing the First 4 Hours (0–4) with the Last 4 Hours (8–12)

Case	PDC (HR level)		PG (ms) at PDC		PVR at PDC		PV(f) (ms) at PDC		PV(s) (ms) at PDC	
	0–4 hr	8–12 hr	0–4 hr	8–12 hr	0–4 hr	8–12 hr	0–4 hr	8–12 hr	0–4 hr	8–12 hr
1	95	85	115	100	1.22	1.16	531	613	646	713
2	110	95	118	161	1.27	1.33	434	490	552	651
3	110	115	104	100	1.24	1.23	434	480	538	580
4	UM	65	0	163	1.00	1.23	UM	711	UM	874
5	100	105	191	191	1.43	1.44	445	431	636	622
6	90	90	241	243	1.54	1.54	449	446	690	689
7	95	85	253	314	1.60	1.69	423	454	676	768
8	100	90	235	294	1.59	1.70	397	419	632	713
9	105	105	140	167	1.30	1.36	463	470	603	637
10	90	85	168	187	1.37	1.36	460	518	628	705
11	85	75	66	133	1.12	1.21	550	639	616	772
12	UM	UM	0	0	1.00	1.00	UM	UM	UM	UM
13	90	80	226	256	1.49	1.52	460	490	686	746
Median	95	87.5	140	167	1.30	1.40	449	485	632	709
Mean (SD)	97 (8)	90 (14)	143 (86)	178 (86)	1.30 (0.2)	1.40 (0.2)	459 (45)	513 (92)	628 (50)	706 (79)
P value	P < .05		P < .05		P < .05		P < .01		P < .01	

HR, heart rate; hr, hours; ms, milliseconds; NS, nonsignificant; PV(f), peak value of the shorter RR-interval population; PV(s), peak value of the longer RR-interval population; PDC, peak dominant change; PG, peak gap; PVR, peak value ratio; SD, standard deviation; UM, unimodal.

at average heart-rate levels ranging from 85 to 110 (0–4 hr) and from 65 to 115 bpm (8–12 hr). The heart-rate level at which the PDC was located decreased from 97 (0–4 hr) to 90 bpm (8–12 hr) ($P < .05$) (Table 3). The PG and PVR increased from 143 ms to 178 ms ($P < .05$) and from 1.30 to 1.40 ($P < .05$), respectively. At the PDC, both the PV(f) and PV(s) were significantly increased, from 459 to 513 ms ($P < .01$) and from 628 to 706 ms ($P < .01$), respectively. The difference in conduction delay between PV(f) (459 to 513) and PV(s) (628 to 706) was 24 ms ($P < .05$).

Blood and Urine Parameters

In the intervention study in group (a), S-Mg increased from 0.94 to 2.18 mmol/L⁻¹ ($P < .01$), and in group (b), from 0.92 to 2.39 mmol/L⁻¹ ($P < .01$). Blood and urine parameters are shown in Table 4.

Discussion

Evidence That the Two RR-Interval Populations Represent a Dual AV-Nodal Conduction System During CAF

A characteristic and highly reproducible RR-interval distribution, with two separate RR-interval populations, is evidenced when HRS analysis is performed during CAF (12,14). The distribution of RR intervals is estimated at well-defined average heart-rate levels (ie, at a distinct balance between

the vagal and the sympathetic nervous discharge). Provided that the RR distribution can be studied over a wide range of average heart-rate levels, the bimodal RR distribution can be found in a majority of patients, consistent with the frequency of dual pathway physiology found in invasive studies (27). That the bimodal RR distribution represents the dual pathway is strongly supported by the fact that interference with conduction along the posterior nodal input via catheter ablation markedly changes the RR distribution pattern (15). In some cases, a third RR population is found at lower heart-rate levels and has been defined as a nodal escape rhythm (12). The two separate RR populations, made up of shorter and longer RR-intervals at heart rate levels above 70 bpm, thus suggest AV-nodal conduction via dual AV-nodal pathways.

The longitudinal dissociation of a slow and a fast pathway within the AV node is well established (1–2,28). Supported by mapping and catheter ablation studies (28–30), it has been proposed that the slow pathway can be attributed to cells with characteristics for slow conduction (17), surrounding the tricuspid annulus in the posterior approaches to the AV node, whereas the fast pathway has been targeted at the anterosuperior perinodal tissue, proximal to the His bundle (31).

It is obvious from RR-interval analysis that a decreased average ventricular rate is achieved by more abundant use of RR intervals within the long RR population, together with a successive and parallel prolongation of all RR intervals of both RR populations, known as rate dependence of peaks (Fig. 3) (14). The successive and parallel changes of all RR intervals could reflect successive changes in

Table 4. Statistical Evaluation of Peak Indices

No. of RR Intervals	PDC		PG		PVR		PV(f)		PV(s)	
	CV (%)	r	CV (%)	r	CV (%)	r	CV (%)	r	CV (%)	r
240	3.0 (1.9)	0.98	20.9 (27.3)	0.98	4.8 (3.2)	0.97	2.6 (1.5)	0.99	3.1 (1.6)	0.98
500	2.4 (1.1)	0.98	14.1 (10.1)	0.96	4.1 (3.1)	0.94	3.1 (3.8)	0.93	3.0 (2.4)	0.99
1,000	2.0 (1.3)	0.98	13.6 (8.8)	0.99	4.2 (3.0)	0.98	2.8 (2.8)	0.97	3.0 (2.4)	1.0
5,000	0.8 (1.4)	0.99	6.8 (4.9)	1.0	2.1 (1.5)	1.0	1.8 (1.3)	1.0	1.3 (1.2)	1.0
20 ²⁰ (24 hr)		0.99		0.99		0.99		1.0		1.0
20 ¹ (24 hr)		1.0		1.0		1.0		1.0		1.0

Coefficients of variance (CV) in percentage, presented as means and standard deviations from the mean [mean (SD)], and correlation (r) between peak indices. Data are derived from histograms constructed using 240, 500, 1,000, 5,000, and all RR intervals, obtained with the pooling procedures of 20¹ (ie, one-by-one step movement) and 20²⁰ (ie, 20-by-20 RR-interval movement) in 8 patients chosen from the control group. The CV was calculated from 3 different analyses, where 240, 500, 1,000, and 5,000 RR intervals were randomly chosen over the whole 24-hour registration period. The correlation between peak indices was calculated for the whole 24-hour interval with the 20¹ pooling procedure and the whole (24 hr) with the 20²⁰ pooling procedure, and from the mean value of 3 different analyses of 240, 500, 1,000, and 5,000 RR intervals randomly chosen over the whole 24-hour registration. This method of heart-rate stratified histogram analysis is a modification of the method used until now. As evidenced by the correlation values, with the new 20¹ pooling procedure, 240 RR intervals were considered sufficient for estimation of peak indices. PDC, peak dominant change; PG, peak gap; PVR, peak value ratio; PV(f), peak value of the shorter RR-interval population; PV(s), peak value of the longer RR-interval population.

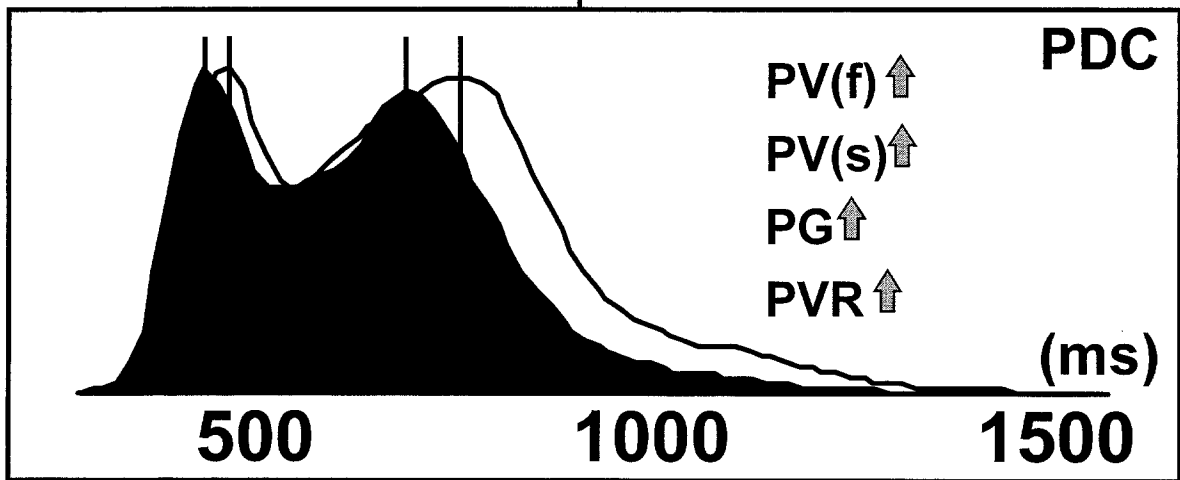
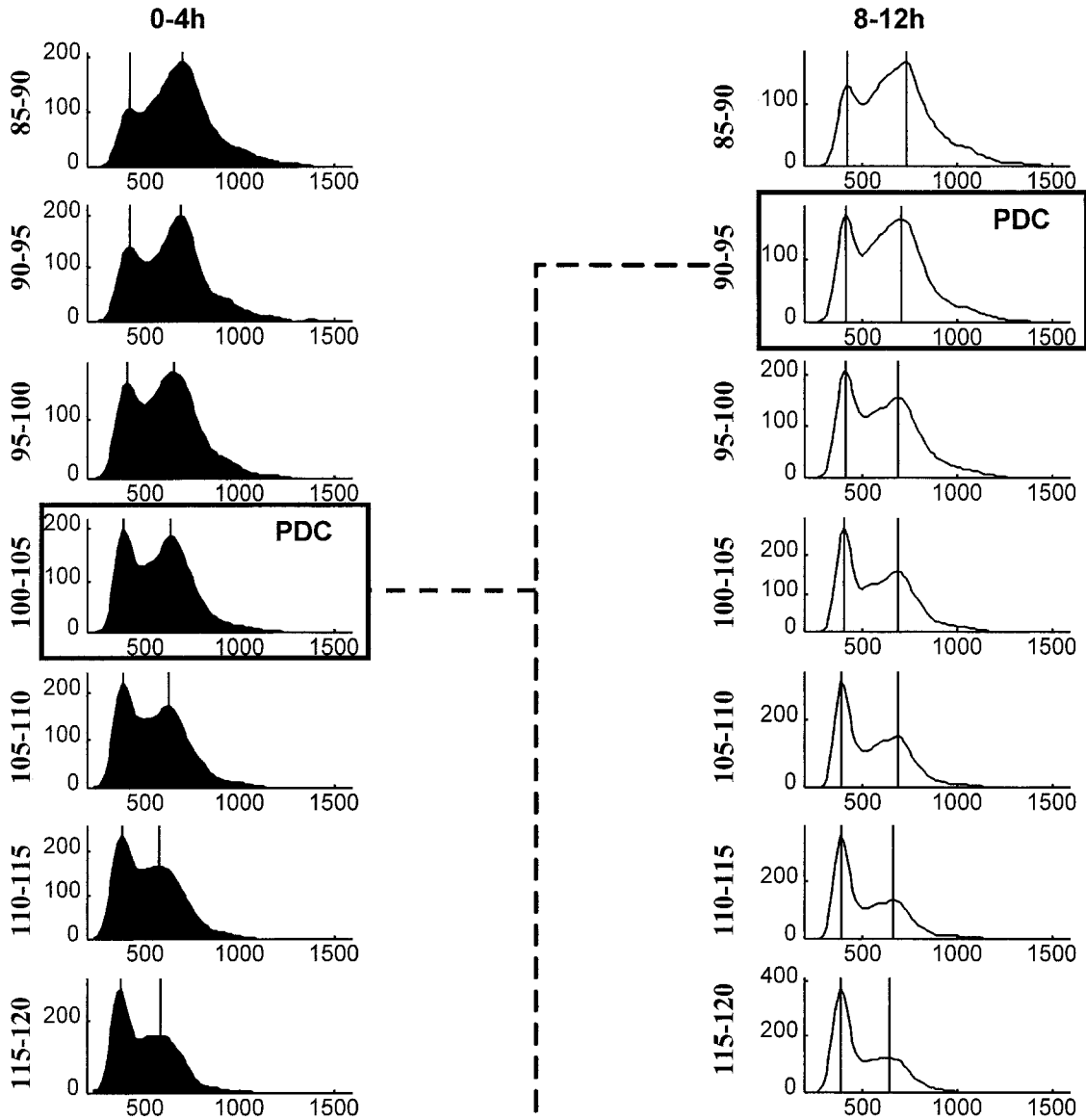


Table 5. Blood and Urine Parameters in Groups (a) and (b)

Parameter Measured	Group (a)			Group (b)			
	Before Inf	12-Hour Inf	24-Hour Inf	Before Inf	MgSO ₄ Bolus Inf	4-Hour Inf	8-Hour Inf
Magnesium (mmol L ⁻¹)	0.94 (0.02)	1.85 (0.06)**	2.18 (0.08)**	0.92 (0.02)	1.60 (0.08)**	2.14 (0.06)**	2.39 (0.12)*
Potassium (mmol L ⁻¹)	4.08 (0.11)	4.09 (0.07)	3.97 (0.15)	4.12 (0.10)	4.11 (0.09)	4.06 (0.10)	4.12 (0.09)
Calcium (mmol L ⁻¹)	2.34 (0.02)	2.17 (0.02)**	2.01 (0.03)**	2.33 (0.03)	2.24 (0.02)**	2.15 (0.03)**	2.03 (0.04)**
Sodium (mmol L ⁻¹)	141 (0.75)	140 (0.65)*	139 (1.02)	142 (0.58)	139 (0.54)**	138 (0.49)	137 (0.53)
Glucose (mmol L ⁻¹)	5.28 (0.47)	4.22 (0.36)	4.06 (0.24)	4.94 (0.36)	7.02 (0.48)**	5.18 (0.32)**	5.55 (0.34)
U-Mg (mmol L ⁻¹)	2.14 (0.22)		21.1 (1.57)				27.0 (3.32)

inf, infusion.

* $P < .05$.** $P < .01$.

conduction and refractory properties within the AV node. The two AV-nodal conduction pathways differ in electrophysiologic characteristics (1–2), the fast pathway being characterized by a longer refractory period and a shorter conduction time, compared with the slow pathway. In the above-mentioned studies (1–2), atrial stimulation was used and the effects of regular or single interpolated stimuli explored. During AF, however, the number of atrial impulses exceeds by far the ventricular response. Fast pathway ablation produces no appropriate decrease in heart rate during AF and has no influence on the global AV-nodal effective refractory period (32), whereas slow pathway ablation decreases the heart rate in AF during rest and autonomic blockade and does not influence the heart rate during exercise and sympathetic stimulation (29). It remains to be verified to what extent the conduction velocity and refractoriness of the different pathways contribute to the specific behavior of the AV-nodal pathways during AF.

Methodological Modification of the HRSH

The newly developed find-peak function made it possible to calculate the histogram peak indices with great precision (Figs. 2, 3). In the method previously used, peak indices were estimated by visual inspection and by manual measurement, and the mean heart rate used for the pooling procedure was calculated

from consecutive sequences of 64 RR intervals (14). In this work, sequences of 20 RR intervals were extracted by one step movement (20¹), using intervals 1–20, 2–21, 3–22, and so on. The number of analyzed 20-interval sequences in a 24-hour registration thus increased from approximately 125 thousand/20 to 2.5 million/20, with an unchanged number of individual RR intervals. The coefficient of variance and correlation for the new 20¹ pooling procedure are illustrated in Table 5. The modified method allowed a more detailed analysis and made it possible to analyze shorter time intervals.

Effects of MgSO₄ and GIK Infusion on the Short and Long RR Populations During CAF

The protocols for groups (a) and (b) were designed to allow the study of short-term effects. However, it was not possible to analyze the effects of MgSO₄ alone in group (b), since the heart-rate variability was too low to provide a sufficient range of average heart-rate levels during the 1-hour study period. Therefore, the RR populations in group (b) were estimated at a lower S-Mg concentration (0–4 hr) and compared with those obtained with MgSO₄ and GIK infusion at a higher S-Mg concentration (8–12 hr), as indicated by the blood parameters (Table 4).

We have recently shown that parenteral adminis-

Fig. 3. A typical example illustrating heart-rate levels between 85 and 120 bpm in one patient in group (b). The first 4 hours (0–4) were compared with the last 4 hours (8–12) of intervention. It is obvious from the histograms that at lower heart-rate levels the longer RR-interval population is dominant, and as the heart rate increases the dominance shifts to the shorter RR population. The peak dominance change, indicated by the framed figures, was shifted to lower heart-rate levels by the MgSO₄ and GIK intervention in group (b). The two superimposed histograms (bottom) illustrate the changes in both RR populations induced by the intervention. The conduction delay in the longer RR population was more pronounced than in the shorter RR population, revealing that the two RR populations were differently affected by the solution that contained a higher MgSO₄ concentration [group (b)].

tration of $MgSO_4$ and GIK solution increases atrial cycle length and decreases heart rate during CAF (24). In this study, the same amount of infusates affected the RR histogram contour by delaying both the shorter and the longer RR populations [group (b)]. The delay in conduction for the longer RR intervals was, however, more pronounced than the delay in conduction for the shorter RR population, as indicated by the difference in conduction delay between PV(f) and PV(s) (24 ms [mean], $P < .05$) and the increased PG and PVR in group (b). There were indications of a similar change in group (a) (low $MgSO_4$ concentration), but only the changes in PG and PV(s) were significant. Because the only difference between the infusates in groups (a) and (b) was a higher $MgSO_4$ concentration in group (b), the conduction delay seems to be caused by $MgSO_4$ alone.

Explanations on the Cellular Level for the Conduction Delay in the Two RR-Interval Populations

The $MgSO_4$ and GIK solution affect at least two different populations of AV-nodal cells (33). The combination of a fast inward current, I_{Na} , and a transient outward current, I_{to} , has been found in 93% of cells with an AN-like structure but in only 24% of cells with an N- or NH-like action potential configuration (33). The myocytes in the AN region seem to be more atriumlike and of fast response type, whereas myocytes in deeper AV-nodal layers (ie, N- or NH-cells) seem to have slow response characteristics.

The two AV-nodal conduction pathways have different electrophysiological characteristics (1–2). This may correspond to different distribution of the different cell populations (17). The fast pathway may have a higher density of myocytes of the fast response type, whereas the slow conduction pathway has a higher density of the slow response type. $MgSO_4$ is a known calcium entry blocker and will decrease the conduction velocity in cells with slow conduction properties (34). However, $MgSO_4$ is also known to decrease potassium conductance, which will increase refractoriness in cells with fast conduction properties (35–36).

There are at least two possible explanations on the cellular level for the $MgSO_4$ effect: (1) the population of longer RR intervals corresponds to the slow pathway and the delay in conduction is caused by a calcium entry blockade that is more pronounced than the increased refractoriness in cells with fast conduction properties, or (2) the population of longer RR intervals corresponds to

the fast pathway and the delay in conduction is caused by an increased refractoriness that is more pronounced than the calcium entry blockade in cells with slow conduction properties.

Alternative Interpretations for the Observed Conduction Delay in the Two RR Populations

Although the findings of this study can thus be explained by a more marked effect of $MgSO_4$ on one of the AV-nodal pathways, other mechanisms cannot be excluded. Others and we have shown that intra-atrial conduction during AF is a nonrandom phenomenon, indicating the possibility of a systematic relationship between the timing of fibrillatory impulses reaching the AV-node from the different atrionodal inputs (37,38). Although there is no report available concerning the interrelationship between time and direction of atrial excitation at different perinodal positions, another plausible interpretation of the $MgSO_4$ effects could be systematic changes in the RR distribution, reflecting a change in timing between the excitation of fibrillatory wavelets at the different atrionodal inputs (ie, the crista terminalis and interatrial septum) (8). Thus, an increase in the atrial fibrillatory cycle length may change the intra-atrial pattern of conduction, resulting in different timing between the excitation of different pathways and thereby in a reshaping of the RR histogram contour (24). This mechanism occurs, for instance, when the global atrial conduction is affected by surgical incision far away from the AV node (13). This alternative explanation of our findings is, however, contradicted by the preliminary report that slow pathway ablation may change a bimodal RR distribution to a unimodal one (15).

Conclusion

Conduction in both the shorter and longer RR populations was delayed by the intervention that had a high $MgSO_4$ concentration. The conduction delay in the longer RR intervals was more pronounced than for the shorter RR intervals. Therefore, we conclude that $MgSO_4$ differently affected the two AV-nodal conduction pathways. A possible interpretation of the results is that the fast and the slow pathways consist of cells with different ion channel densities.

Acknowledgment

This work was supported by grants from the Swedish Heart Lung Foundation and the Medical Faculty, University of Lund, Sweden.

References

- Moe GK, Preston JB, Burlington H: Physiologic evidence for a dual A-V transmission system. *Circ Res* 4:357-375, 1956
- Mendez C, Moe GK: Demonstration of a dual A-V nodal conduction system in the isolated rabbit heart preparation. *Circ Res* 19:378-393, 1966
- Rosen KM, Denes P, Wu D, Dhingra C: Electrophysiological diagnosis and manifestation of dual A-V nodal pathways. p. 453-466. In: Wellens HJJ, Lie KI, Janse MJ (eds). *The Conduction System of the Heart*. The Hague: Martinus Nijhoff, 1978
- Janse MJ: The role of the atrioventricular node in atrial fibrillation. pp. 127-140. In: Olsson SB, Allessie MA, Campbell RWF (eds). *Atrial Fibrillation: Mechanisms and Therapeutic Strategies*. Armonk, NY: Futura Publishing Co, 1994
- Page RL, Wharton JM, Prystowsky EN: Effect of continuous vagal enhancement on concealed conduction and refractoriness within the atrioventricular node. *Am J Cardiol* 77:260-265, 1996
- Zipes DP, Mendez C, Moe GK: Evidence for summation and voltage dependency in rabbit atrioventricular nodal fibers. *Circ Res*, 32:170-177, 1973
- Prystowsky EN, Page RL: Electrophysiology and autonomic influences of the human atrioventricular node. pp. 259-277. In: *Electrophysiology of the Sino-Atrial and Atrioventricular Nodes*. New York: Alan R. Liss, Inc, 1988
- Janse MJ, Van Capelle FJL, Anderson RH, et al: Electrophysiology and structure of the atrioventricular node of isolated rabbit heart. *Am J Physiol* 243H:754-760, 1982
- Janse MJ: Influence of the direction of atrial wave front on AV nodal transmission in isolated hearts of rabbits. *Circ Res* 25:439-449, 1969
- Amat-y-Leon F, Denes P, Wu RJ: Effects of atrial pacing site on atrial and atrioventricular nodal function. *Br Heart J* 37:576-582, 1975
- Batsford WP, Akhtar M, Caracta AR: Effect of atrial stimulation site on the electrophysiological properties of the atrioventricular node in man. *Circulation* 50:283-292, 1974
- Olsson SB, Cai N, Dohnal M, Talwar KK: Noninvasive support for and characterization of multiple intranodal pathways in patients with mitral valve disease and atrial fibrillation. *Eur Heart J* 7:320-333, 1986
- Olsson SB, Cai N, Dohnal M, William-Olsson G: Effect of crista terminalis myotomy on the AV nodal function in atrial fibrillation. pp. 249-261. In: Attuel P, Coumel P, Janse MJ (eds). *The Atrium in Health and Disease*. Mount Kisco, NY: Futura Publishing Company, Inc, 1989
- Cai N, Dohnal M, Olsson SB: Methodological aspects of the use of heart rate stratified RR interval histograms in the analysis of atrioventricular conduction during atrial fibrillation. *Cardiovasc Res* 21:455-462, 1987
- Gaitanidou S, Rokas S, Chatzidou S, et al: The presence of dual atrioventricular node physiology in patients with chronic atrial fibrillation. Clinical implications. *Eur Heart J* 18:P1797, 1997
- Toivonen L, Kadish A, Kou W, Morady F: Determinants of the ventricular rate during atrial fibrillation. *JACC* 16:1194-1200, 1990
- McGuire MA, De Bakker JMT, Vermeulen JT, et al: Atrioventricular junctional tissue: Discrepancy between histological and electrophysiological characteristics. *Circulation* 94:571-577, 1996
- Tieleman RG, De Langen CDJ, Van Gelder IC, et al: Verapamil reduces tachycardia-induced electrical remodeling of the atria. *Circulation* 95:1945-1953, 1997
- Tieleman RG, Crijns HJGM, Van Gelder IC, et al: A clinical illustration of reduction of electrical remodeling by the use of intracellular calcium lowering drugs during AF. *PACE* 20(A):1142, 1997
- Mary-Rabine L, Albert A, Pham TD, et al: The relationship of human atrial cellular electrophysiology to clinical function and ultrastructure. *Circ Res* 52:188-199, 1983
- Ten Eick RE, Singer DH: Electrophysiological properties of diseased human atrium. I. Low diastolic potential and altered cellular response to potassium. *Circ Res* 44:545-557, 1979
- Rosen MR: Editorial comments. pp. 163-169. In: DiMarco JP, Prystowsky EN (eds): *Atrial Arrhythmias: State of the Art*. Armonk, NY: Futura Publishing Co, Inc, 1995
- Ingemansson MP, Carlson J, Platonov P, Olsson SB: Effects of MgSO₄ and glucose, insulin and potassium (GIK) on atrial conduction during the first 12 hours after DC-conversion of chronic atrial fibrillation. (Submitted), 1998
- Ingemansson MP, Smideberg B, Olsson SB: Intravenous MgSO₄ alone and in combination with the hyperpolarising solution (GIK) prolongs the atrial cycle length in chronic atrial fibrillation. *J Cardiovasc Pharmacol* (in press), 1998
- Rasmussen HS, Thomsen PE: The electrophysiological effects of intravenous magnesium on human sinus node, atrioventricular node, atrium, and ventricle. *Clin Cardiol* 12(2):85-90, 1989
- Sodi-Pallares D, Bisteni A, Medrano GA, Testelli MR, De Micheli A. The polarizing treatment of acute myocardial infarction. *Dis Chest* 4:424-432, 1963
- Brugada P, Roy D, Weiss J, Dassen WRM, Wellens HJJ: Dual atrioventricular nodal pathways and atrial fibrillation. *PACE* 7:240-247, 1984

28. Keim S, Werner P, Jazayeri M, Akhtar M, Tchou P: Localisation of the fast and slow pathways in atrioventricular nodal reentrant tachycardia by intraoperative ice mapping. *Circulation* 86:919–925, 1992
29. Strickberger SA, Weiss R, Daoud EG, et al: Ventricular rate during atrial fibrillation before and after slow-pathway ablation. *Circulation* 94:1023–1026, 1996
30. Haissaguerre M, Gaita F, Fischer B, et al: Elimination of atrioventricular nodal reentrant tachycardia using discrete slow potentials to guide application of radiofrequency energy. *Circulation* 85:2162–2175, 1992
31. Langberg JJ: Radiofrequency catheter ablation of AV nodal reentry: The anterior approach. *PACE* 16:615–622, 1993
32. Duckeck W, Engelstein ED, Kuck KH: Radiofrequency current therapy in atrial tachyarrhythmias: Modulation versus ablation of AV nodal conduction. *PACE* 16:629–636, 1993
33. Munk AA, Adjemian RA, Zhao J, Ogbaghebriel A, Shrier A: Electrophysiological properties of morphologically distinct cells isolated from the rabbit atrioventricular node. *J Physiol (Lond)* 15:801–818, 1996
34. Hess P, Lansman JB, Tsien RW: Calcium channel selectivity for divalent and monovalent actions. *J Gen Physiol* 88:293–318, 1986
35. Biermans G, Vereecke J, Carmeliet E: The mechanism of the inactivation of the inward-rectifying K current during hyperpolarizing steps in guinea-pig ventricular myocytes. *Pflügers Arch* 410:604–613, 1987
36. Zhang S, Sawanobori T, Adaniya H, Hirano Y, Hiraoka M: Dual effects of external magnesium on action potential duration in guinea pig ventricular myocytes. *J Am Physiol Soc* H2321–H2328, 1995
37. Holm M, Johansson R, Brandt J, Luhrs C, Olsson SB: Epicardial right atrial free wall mapping in chronic atrial fibrillation. Documentation of repetitive activation with a focal spread—a hitherto unrecognised phenomenon in man. *Eur Heart J* 18: 290–310, 1997
38. Gerstenfeld EP, Sahakian AV, Swiryn S: Evidence for transient linking of atrial excitation during atrial fibrillation in humans. *Circulation* 86:375–382, 1992